



Table 2: List of PNe in the direction of the galactic bulge with 8-13 $\mu$ m spectra, and the identified warm dust emission features.

| PN G               | dust type   | N/O type | He <sup>a</sup> | N <sup>a</sup> | O <sup>a</sup> | $V_{\text{lsr}}$<br>km s <sup>-1</sup> | $d$<br>kpc | bulge PN? <sup>b</sup> | ref <sup>c</sup> | comments <sup>h</sup> |   |
|--------------------|-------------|----------|-----------------|----------------|----------------|--|------------|------------------------|------------------|-----------------------|---|
| H1-54              | 2.1 – 4.2   | O        | IIb             | 10.99          | 7.48           | 8.56                                   | -116       | 11.4                   | AB               | 4;2                   | silicates:1,191                                   |
| M2-23              | 2.2 – 2.8   | O        | IIb             | 10.98          | 7.40           | 8.22                                   | 186        | 8.4                    | AB               | 1;2                   | silicates <sup>e</sup>                            |
| H1-63              | 2.3 – 6.4   | O        | x               | -              | -              | -                                      | -1.0       | <5.7                   |                  | 4;6                   | silicates:1,195                                   |
| Cn1-5              | 2.3 – 9.5   | C        | IIa             | 11.06          | 8.63           | 9.05                                   | -29.7      | 4.4                    |                  | 4;2                   | graphite:0.15,130 UIR:0.58,0.15,0.12              |
| M1-38              | 2.5 – 3.7   | C        | IIb             | 11.04          | 8.21           | 9.00                                   | -70.0      | 6.6                    | AB               | 4;2                   | graphite:0.4,144 UIR:—,0.3,0.3                    |
| M1-37              | 2.6 – 3.4   | +        | I               | 11.10          | 8.10           | 7.98                                   | 220        | 8.1                    | AB               | 1;1                   | weak continuum <sup>e</sup>                       |
| M1-35              | 3.9 – 2.3   | +        | I               | 11.35          | 8.79           | 8.48                                   | 67.4       | 4.6                    |                  | 1;2                   | weak continuum                                    |
| M2-29 <sup>d</sup> | 4.1 – 3.0   | O        | IIa             | 11.11          | 7.01           | 7.47                                   | -112       | 9.9                    | AB               | 1;2                   | silicates:1,215                                   |
| H1-53              | 4.3 – 2.6   | O        | x               | -              | -              | -                                      | 75.0       | -                      |                  | 4;5                   | silicates:1,199                                   |
| M1-25              | 4.9 + 4.9   | +        | I               | 11.10          | 8.82           | 9.09                                   | 14.1       | 4.9                    |                  | 1;2                   | weak continuum                                    |
| M1-20              | 6.2 + 8.4   | c        | IIb             | 11.02          | 7.75           | 8.62                                   | 60.3       | 5.9                    |                  | 1;2                   | graphite:0.6,191 SiC:0.4,120                      |
| M3-15              | 6.8 + 4.1   | +        | IIa             | 11.03          | 8.14           | 8.74                                   | 97.5       | 4.1                    |                  | 1;2                   | weak continuum                                    |
| NGC6644            | 8.3 – 7.3   | +        | IIa             | 11.03          | 8.00           | 8.54                                   | 194        | 4.1                    | A                | 4;2                   | weak continuum <sup>e</sup>                       |
| M3-21              | 355.1 – 6.9 | +        | IIa             | 11.05          | 8.26           | 8.74                                   | -66.1      | 5.6                    |                  | 1;2                   | weak continuum                                    |
| H1-32              | 355.7 – 2.7 | O        | IIa             | 10.95          | 7.59           | 8.12                                   | -222       | -                      | A                | 3;-                   | silicates:1,228                                   |
| M1-27              | 356.5 – 2.4 | C        | IIb             | -              | 8.22           | 8.86                                   | -49.7      | 3.7                    |                  | 1;2                   | graphite:0.6,220 SiC:0.4,194 <sup>f</sup>         |
| M2-24              | 356.9 – 5.8 | +        | x               | -              | -              | -                                      | 145.5      | -                      | A                | 7;-                   | unidentified <sup>g</sup>                         |
| M3-38              | 357.0 + 4.4 | O        | I               | 11.11          | 8.69           | 8.37                                   | -156       | 8.3                    | AB               | 4;2                   | graphite:0.21,296 silicates:0.52,152 UIR:—,—,0.27 |
| M3-8               | 358.2 + 4.3 | O        | I               | 11.11          | 8.75           | 9.02                                   | 95.0       | 7.5                    | AB               | 4;2                   | silicates:1,291                                   |
| M4-6               | 358.6 + 1.8 | +        | IIb             | 10.98          | 7.97           | 8.31                                   | -292       | 6.3                    | AB               | 4;2                   | weak continuum <sup>e</sup>                       |
| Th3-26             | 358.8 + 3.0 | +        | x               | -              | -              | -                                      | 204        | 7.9                    | AB               | 4;2                   | weak continuum                                    |
| M1-29              | 359.1 – 1.7 | +        | I               | 11.14          | 8.82           | 9.00                                   | -41.3      | 3.3                    |                  | 1;2                   | weak continuum                                    |
| M3-44              | 359.3 – 1.8 | +        | x               | -              | -              | -                                      | -89.0      | >1                     | A                | 4;6                   | weak continuum <sup>e</sup>                       |
| H1-40              | 359.7 – 2.7 | O        | IIa             | 11.06          | 8.08           | 8.70                                   | 63.8       | 7.8                    | AB               | 1;1                   | silicates <sup>e</sup>                            |
| M2-27              | 359.9 – 4.5 | +        | IIa             | 11.07          | 8.46           | 8.77                                   | 145        | 5.7                    | A                | 1;2                   | weak continuum <sup>e</sup>                       |

<sup>a</sup> The abundances were taken from Ratag et al. (1997), except for M1-27 which is from Cuisinier et al. 2000.

<sup>b</sup> Criteria met for bulge membership (see text).

<sup>c</sup> References for measurements of  $V_{\text{lsr}}$  and estimates of the distance respectively. The codes are: 1) Zijlstra, Acker & Walsh (1997); 2) Zhang (1995); 3) Kohoutek and Pauls (1995); 4) Schneider et al. (1983); 5) Acker et al. (1991); 6) Maciel (1984); 7) Durand, Acker & Zijlstra (1998).

<sup>d</sup> The abundances for M 2-29 are uncertain: The analysis by Torres-Peimbert et al. (1997) suggests previously reported [O/H] values are underestimated.

<sup>e</sup> 8–13  $\mu$ m spectra from Roche (1987).

<sup>f</sup> The fit to M1-27 with SiC and graphite had  $\chi^2=1.03$ , while graphite alone gave  $\chi^2=1.9$ , and a trapezium emissivity function resulted in  $\chi^2=2.5$ .

<sup>g</sup> M 2-24's 8–13  $\mu$ m spectrum is atypical of PNe (compare with K 4-57 in paper I).

<sup>h</sup> Best fit parameters for the 8–13 $\mu$ m continua: (graintype): $a', T$  for SiC or silicates, where  $a'$  is the relative contribution and  $T$  the temperature of the modified black body corresponding to (graintype); UIR: $a'_{7.7}, a'_{8.6}, a'_{11.3}$  for the unidentified IR bands (see Section 2 for more details).

# 8–13 $\mu$ m Dust Emission Features in Galactic Bulge Planetary Nebulae

S. Casassus<sup>1,2</sup>, P. F. Roche<sup>1</sup>, D. K. Aitken<sup>3</sup> & C. H. Smith<sup>4</sup>

<sup>1</sup> *Astrophysics, Physics Department, Oxford University, Keble Road, Oxford OX1 3RH*

<sup>2</sup> *Departamento de Astronomía, Universidad de Chile, Casilla 36-D, Santiago, Chile.*

<sup>3</sup> *Department of Physical Sciences, University of Hertfordshire, Hatfield, Herts AL10 9AB*

<sup>4</sup> *School of Physics, University College, UNSW, Canberra, ACT 2600, Australia.*

Accepted ... Received ...

## ABSTRACT

A sample of 25 IR-bright planetary nebulae (PNe) towards the Galactic bulge is analysed through 8–13 $\mu$ m spectroscopy. The classification of the warm-dust emission features provides a measure of the C/O chemical balance, and represents the first C/O estimates for bulge PNe. Out of 13 PNe with identified dust types, 4 PNe have emission features associated with C-based grains, while the remaining 9 have O-rich dust signatures. The low fraction of C-rich PNe,  $\lesssim 30\%$ , contrasts with that for local PNe, around  $\sim 80\%$ , although it follows the trend for a decreasing frequency of C-rich PNe with galactocentric radius (paper I). We investigate whether the PNe discussed here are linked to the bulge stellar population (similar to type IV, or halo, PNe) or the inner Galactic disk (a young and super-metal-rich population). Although 60% of the PNe with warm dust are convincing bulge members, none of the C-rich PNe satisfy our criteria, and they are probably linked to the inner Galactic disk. In the framework of single star evolution, the available information on bulge PNe points towards a progenitor population similar in age to that of local PNe (type I PNe are found in similar proportions), but super-metal-rich (to account for the scarcity of C-rich objects). Yet the metallicities of bulge PNe, as inferred from [O/H], fail to reach the required values - except for the C-rich objects. It is likely that the sample discussed here is derived from a mixed disk/bulge progenitor population and dominated by type IV PNe, as suggested by Peimbert (1992). The much higher fraction of O-rich PNe in this sample than in the solar neighbourhood should result in a proportionally greater injection of silicate grains into the inner Galactic medium.

**Key words:** planetary nebulae: general – infrared: ISM: lines and bands – ISM: abundances – stars: evolution – stars: AGB and post-AGB.

## 1 INTRODUCTION.

Planetary nebula (PN) compositions reflect the initial composition and nuclear processing undergone by their progenitors, and provide valuable information on the end point of evolution for populations of intermediate mass stars in various galactic environments. Ratag et al. (1997) have published an extensive abundance analysis of PNe towards the Galactic bulge, providing helium, oxygen and nitrogen abundances. The results are surprising as many bulge PNe have high N/O ratios, which is characteristic of Peimbert type I PNe. The temptation to link the high N/O ratio in the bulge with the high progenitor masses of type I PNe, in excess of 2–3 $M_{\odot}$ , is countered by growing evidence that the bulge

and halo are coeval (Ortolani 1995). In an addendum to his review on PNe, Peimbert (1992) favours a link with halo PNe (type IV, defined by a very low metallicity), which sometimes have N/O ratios within the range of type I PNe. However, carbon is conspicuously absent from the previous abundance analyses, and the C/O chemical balance is also a function of progenitor mass.

The C/O abundance ratio in PNe is usually calculated from gas phase abundances, through fine structure emission lines of C and O ionised up to three times. But the bright C lines are [C II]  $\lambda 2326$ , [C III]  $\lambda 1908$ , [C IV]  $\lambda 1550$ , and extinction is severe at such short wavelengths. As the lines of sight to the bulge are usually affected by strong extinction, no C abundances are available for bulge PNe. However, the C/O chemical balance

can be inferred from the 8–13 $\mu\text{m}$  warm dust signatures, through the identification of the grain type. Silicate emission corresponds to oxygen-rich environments, SiC emission is typical of carbon-rich environments, while the unidentified infrared (UIR) emission bands are associated with a strong overabundance of carbon relative to oxygen (e.g. Barlow 1983, Roche 1989, see also Casassus et al. 2001a, paper I).

In this article we analyse a sample of bulge PNe through their dust signatures. We present 8–13 $\mu\text{m}$  spectra for a sample of 18 PNe observed towards the Galactic bulge (which meet the bulge-membership criteria of Acker et al. 1991), and analyse these, together with 7 objects previously reported by Roche (1987). We determine the dominant dust emission features in terms of grain emissivities, thus deriving the C/O chemical balances. Section 2 contains a description of the observations. A compilation of the data available for the sample of bulge PNe with 8–13 $\mu\text{m}$  spectra, together with a discussion on the criteria for bulge membership, is presented in Section 3. In Section 4 we interpret the available information on bulge PNe. In the framework of single star evolution, the rarity of C-rich PNe and the high frequency of N-enrichment links the ‘bulge’ PNe with the inner Galactic disk rather than with the bulge stellar population. But the O abundances in bulge PNe do not reach the required super-metal-rich values. The failure of single star evolution models in accounting for bulge PNe is thus highlighted. Section 5 summarises our conclusions.

## 2 8–13 $\mu\text{m}$ SPECTRA OF PNE TOWARDS THE GALACTIC BULGE

The objects selected were required to satisfy the following criteria,

- good detection by *IRAS* at 25  $\mu\text{m}$ , and 12  $\mu\text{m}$  flux in excess of  $\gtrsim 0.5$  Jy, or high upper limits,
- diameters less than 10'', and almost all  $< 5''$ ,
- listed as likely bulge PNe in the Strasbourg-ESO catalogue (Acker et al. 1992), i.e.  $-10 < l < 10$ ,  $-10 < b < 10$ ,  $F(6\text{ cm}) < 100$  mJy.

The spectra were acquired during July 23–26 1990, using UCLS at UKIRT, with the 40 l/mm grating and an aperture of 4.5 arcsec in diameter. The linear array of 25 Si:As photoconductive detectors was oversampled two times. Flux calibration was relative to standard stars and is accurate to 20%, and Table 1 contains a list of the observed PNe, as well as the emission line fluxes.

Fig. 1 shows the resulting spectra, together with the fits based on the different grain emissivities, according to the procedure from Aitken et al. (1979), and also described in paper I. Table 2 lists the warm dust identification for the 25 bulge PNe which have been observed spectroscopically at 8–13 $\mu\text{m}$  (henceforth the bulge PN

Table 1: List of objects observed with UCLS at UKIRT in July 1990. Emission line fluxes are  $10^{-15}$   $\text{W m}^{-2}$

|        | PNG       | [Ar III]<br>8.99 $\mu\text{m}$ | [S IV]<br>10.52 $\mu\text{m}$ | [Ne II]<br>12.81 $\mu\text{m}$ |
|--------|-----------|--------------------------------|-------------------------------|--------------------------------|
| H1-54  | 2.1–4.2   | —                              | —                             | 1.7                            |
| H1-63  | 2.2–6.3   | —                              | —                             | 0.5                            |
| Cn1-5  | 2.2–9.4   | 0.7                            | 2.0                           | 1.2                            |
| M1-38  | 2.4–3.7   | —                              | —                             | 3.9                            |
| M1-35  | 3.9–2.3   | 1.8                            | 8.7                           | 1.0                            |
| M2-29  | 4.0–3.0   | —                              | 0.4                           | —                              |
| H1-53  | 4.3–2.6   | 1.4                            | 1.5                           | 1.7                            |
| M1-25  | 4.9+4.9   | 2.0                            | —                             | 8.6                            |
| M1-20  | 6.1+8.3   | 0.7                            | 1.2                           | —                              |
| M3-15  | 6.8+4.1   | 1.3                            | 4.9                           | —                              |
| M3-21  | 355.1–6.9 | 0.8                            | 7.3                           | —                              |
| H1-32  | 355.6–2.7 | —                              | 0.9                           | —                              |
| M1-27  | 356.5–2.3 | —                              | —                             | 5.8                            |
| M2-24  | 356.9–5.8 | —                              | —                             | —                              |
| M3-38  | 356.9+4.4 | —                              | 2.2                           | 0.3                            |
| M3-8   | 358.2+4.2 | 0.6                            | 1.0                           | 0.9                            |
| Th3-26 | 358.8+3.0 | —                              | 3.3                           | —                              |
| M1-29  | 359.1–1.7 | 1.9                            | 3                             | 0.7                            |

sample). The spectra for PNe in Table 2 which are not listed in Table 1 are published in Roche (1987). The column under ‘comments’ contains the best fit parameters to the 8–13 $\mu\text{m}$  continua, with the notation of paper I, leading to a classification of dust signatures in terms of the dominant component (see Table 3 in paper I):

$$F_\lambda = \sum_i a_i \epsilon_i(\lambda) B(\lambda, T_i) / B(10\mu\text{m}, T_i), \quad (1)$$

where we sum over grain types, each with an emissivity  $\epsilon_i$ , and where  $B(\lambda, T_i)$  is a Planck function at temperature  $T_i$ . The free parameters are  $a_i$  and  $T_i$ , the relative contribution of each grain type being  $a'_i = a_i / \sum_j a_j$ . In this classification, a superposition of silicate emission and the UIR bands is classified as O-rich, because all ‘O’ PNe classified in this way have gas phase C/O  $< 1$  (in the sample discussed here, only M3-38 shows such a superposition).

The proportion of PNe with C-based grains is smaller for PNe with longitudes towards the bulge than in the disk population:

|  | Bulge         | Disk            |               |
|--|---------------|-----------------|---------------|
|  |               | $R < R_\odot^a$ | $R > R_\odot$ |
|  | $31 \pm 13\%$ | $70 \pm 9\%$    | $86 \pm 7\%$  |

<sup>a</sup>  $R_\odot = 8.5$  kpc corresponds to the solar circle (Kerr & Lynden-Bell 1986).

There is a striking difference between the bulge PN sample compared with local PNe (see paper I for a discussion on the dust signatures in local PNe). This may be interpreted either as support for linking the PNe in Table 2 with the bulge stellar population, or as a strong metallicity dependence in the PN compositions. By contrast central star properties (Tyndal et al. 1991), or other nebular abundances (Section 3 below), have not

Landscape Table to go here

Table 2:

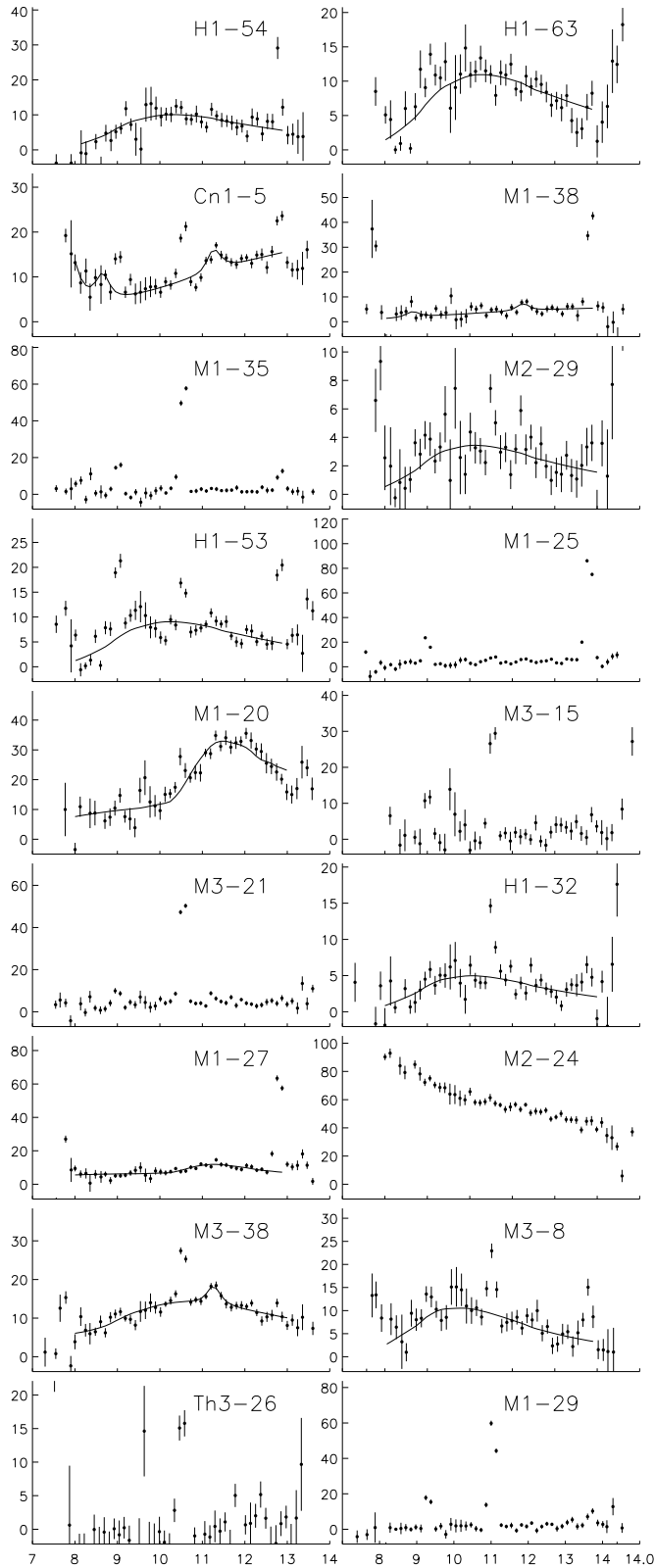


Figure 1:  $10\mu\text{m}$  spectra of the PNe listed in Table 1. The abscissae are the wavelengths in  $\mu\text{m}$ , and the ordinates the flux density in  $10^{-15}\text{W m}^{-2}\mu\text{m}^{-1}$ . Fits to the dust emission continua are shown by the solid lines (fit parameters are in Table 2). Bright emission lines of [A III], [S IV] or [Ne II] at 9.0, 10.5 and  $12.8\mu\text{m}$  are excluded from the fitting procedure.

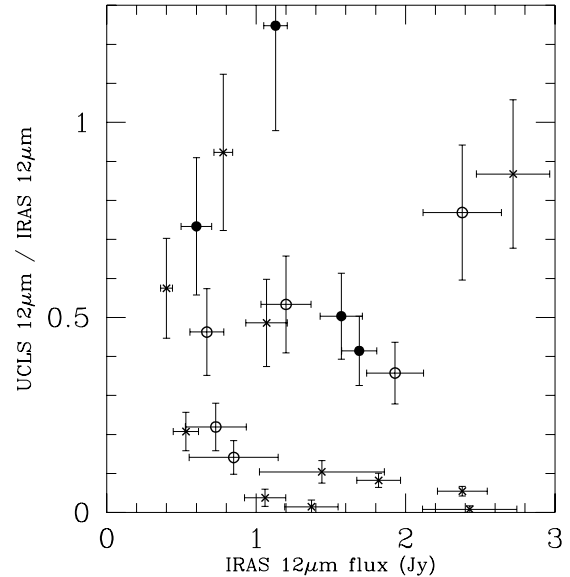


Figure 2: The ratio of UCLS to *IRAS*  $12\mu\text{m}$  flux as a function of *IRAS* flux. Open and filled circles correspond to O-rich and C-rich objects respectively, while crosses denote weak continuum PNe.

convincingly been demonstrated to reflect the broadly varying bulge and local galactic environments.

Does the IR-bright selection criterion preferentially select silicate nebulae? As shown in paper I, the fraction of flux emitted in the  $12\mu\text{m}$  band,  $F(12\mu\text{m})/F_{\text{IRAS}}$ , is about 25% and independent of dust emission type. No particular bias towards silicate nebulae is expected, and moreover the bulge sample is subject to the same selection effects as the disk sample in paper I. In spite of a lower  $F(12\mu\text{m})/F_{\text{IRAS}}$  of  $\sim 10\%$ , ‘weak’ nebulae are found in a proportion of 48% in the bulge sample, against 27% in the disk. The higher proportion of ‘weak’ nebulae is probably because the Galactic bulge sample is at a greater average distance from the sun, and hence fainter than the disk sample, but also many bulge PNe have upper limits only in the  $12\mu\text{m}$  band.

It is noteworthy that the  $11\text{--}13\mu\text{m}$  flux measured from the ground with the UCLS is in many cases substantially lower than that measured by *IRAS*. The average  $12\mu\text{m}$  flux ratio is 0.36, but this varies from 0.67 for C-rich objects, 0.48 for O-rich objects and 0.17 for PNe with weak continua, as shown in Fig. 2 (objects with *IRAS* upper limits at  $12\mu\text{m}$  are excluded, but those with uncertain detections are included). While source extension beyond the UCLS aperture and pointing errors may account for some of this difference, it seems that in the objects with weak continua, line emission and/or very strongly-rising continua beyond  $13\mu\text{m}$  must provide the bulk of the emission, if the  $12\mu\text{m}$  *IRAS* fluxes are accurate in this crowded region.

### 3 BULGE MEMBERSHIP AND GAS PHASE ABUNDANCES

Due to the lack of accurate distance indicators for PNe, bulge membership cannot be determined with certainty, but it is strengthened if the following criteria are met:

- Criterion A. The bulge is the site of large velocity dispersions, in contrast to the near-circular orbits in the Galactic disk. If a PN is associated with the Galactic disk, the maximum line of sight velocity towards the bulge would be of the order of the velocity dispersion for  $1 M_{\odot}$  stars in the solar neighbourhood, or about  $\sigma \sim 80 \text{ km s}^{-1}$  (from the age-velocity dispersion relation in Wielen 1977). In the extreme case of placing the PNe on the inner side of the molecular ring (galactocentric radius  $R \sim 2.5 \text{ kpc}$ ), bulge membership is strengthened if the deviation from circular rotation is greater than  $\sigma$ .

- Criterion B. PNe with distances beyond 6 kpc are bulge members. When available, we used the statistical distances from Zhang (1995), which are averaged between an ionised mass-radius distance scale, and that in van de Steene & Zijlstra (1995), based on a brightness temperature  $T_b(6 \text{ cm})$ –radius relationship. Otherwise we used the distances from van de Steene and Zijlstra (1995), or the distances computed by Maciel (1984, based on the mass-radius relation). In the case of H1-53, only the Acker et al. (1991) criterion for bulge membership is available (although H1-53 has an undefined angular size and the flux reported is at 2 cm).

The  $D_{IRAS}$  distances discussed in paper I, based on a constant PN luminosity of  $8500 L_{\odot}$  and using the 4 *IRAS* bands to approximate the bolometric flux, cannot be used to identify bulge members because of poor quality *IRAS* fluxes. However, the assumption that 50% of the bolometric flux falls in the  $25\mu\text{m}$  band ( $0.52 \pm 0.1$  in the sample of paper I) yields estimated  $D_{IRAS}$  distances that correlate well with the values in Table 2. The ratio of  $D_{IRAS}$  to 6 cm-based distances is 1.9 with a  $1\sigma$  spread of 0.6. The same ratio is  $1.8 \pm 0.8$  in the sample of Galactic disk PNe with warm dust emission. It is interesting to note that, for PNe which are optically thick to their nuclei’s radiation, the approximation of constant luminosity gives distances which are in excess of 6 cm-based distances *by the same factor* for bulge and disk objects, thereby hinting at similar PN bolometric luminosity functions (LFs) for the two populations. Perhaps this is related to the constancy of the [O III] PNLF in broadly varying galactic environments (Ciardullo et al. 1991)?

Of the C-rich objects, only M1-38 satisfies criteria A and B for bulge membership, and its dust signature is rather uncertain. M3-38 shows a superposition of silicate and UIR emission, and it is classified as an ‘O’ type PN with the definitions of Table 3 in paper I. We stress that this convention follows the gas-phase abundances, ‘O’ PNe are also O-rich, although there are only

two objects with such a superposition and known C/O ratio. Ratag et al. (1997) report a high N/O ratio for M3-38.

Table 2 also contains a summary of the observational data on bulge PNe with 8–13 $\mu\text{m}$  spectra. Nitrogen enrichment is classified according to Peimbert (1978), with the sub-types from Faundez-Abans and Maciel (1987) but without the kinematical distinctions (i.e.  $\log(\text{N/O}) > -0.3$  in type I PNe,  $-0.3 > \log(\text{N/O}) > -0.6$  in type IIa PNe, and  $-0.6 > \log(\text{N/O})$  in type IIb PNe), and the gas-phase abundances are mostly taken from Ratag et al. (1997). Note however that the agreement between different data sets for the few objects in common (Ratag et al 1997, Cuisinier et al 2000, Webster 1988), which are generally faint and reddened, is rather poor. There appears to be a high proportion of type I PNe in the bulge sample, 25% of the total, or 30% of the PNe which satisfy criteria A and B for bulge membership. This value is close to the proportion of type I PNe in compact and infrared bright Galactic disk PNe,  $29 \pm 6\%$ . Cuisinier et al. (2000) obtain similar distributions for N/O ratios in bulge and local PNe, considering the small number statistics. In fact, although their interpretation points towards a marked difference with local PNe, their data shows 23% type I objects, and with a continuous range of N/O values, like the Galactic disk PNe. There is also a large population of type IIa nebulae in the bulge, 33% in this sample, compared to  $\sim 12\%$  in the disk (in the sample of paper I).

As an example of the uncertainties affecting the gas phase abundances, consider the case of M 2-29: ground based spectra yielded  $[\text{O/H}] = -1.4$  dex, making M 2-29 the most metal poor PN so far, but Torres-Peimbert et al. (1997) reported  $[\text{O/H}] = -0.5$  dex from HST FOS spectra of a knot close to the central star. Are the HST results typical of the whole nebula? Would density and temperature inhomogeneities also affect the abundance determinations of other bulge PNe? Although we will consistently refer to the work by Ratag et al. (1999), the gas-phase abundances can only be viewed as rough indicators.

The distribution of oxygen abundances listed in Table 2, for the 10 objects with warm dust emission and known  $[\text{O/H}]$ , is  $[\text{O/H}] = -0.3 \pm 0.4$  dex\* (in terms of the mean and  $1\sigma$  spread and for a solar abundance of  $7.4 \cdot 10^{-4}$ , Grevesse & Anders 1989). In the Galactic disk PNe discussed in paper I, the distribution of oxygen abundances for the objects with warm dust emission, is  $[\text{O/H}] = -0.52 \pm 0.26$  dex for  $R > R_{\odot}$ ,

\* Note we average logarithmic abundances, so as to avoid negative values when characterising the distribution of linear abundance values. The drawback is an ‘inflating’ effect, in this case taking the log of the linear average of O abundances would give  $[\text{O/H}] = -0.15$ . In this respect we follow McWilliam & Rich (1994), and the same procedure is used in papers I and II.

$[O/H] = -0.22 \pm 0.21$  dex for  $R < R_\odot$ , and  $[O/H] = -0.31 \pm 0.26$  dex for all  $R$ . Thus the mean  $[O/H]$  in bulge and local PNe is very similar, and even if the spread in  $[O/H]$  is larger for bulge PNe, the maximum and minimum observed values are comparable to local PNe: From  $[O/H] \sim -1$  dex to  $[O/H] \sim +0.2$  dex. The distribution of  $[O/H]$  values for the PNe discussed here is very similar to the distribution of  $[Fe/H]$  in Baade's window K giants,  $\sim 1$  dex about  $\langle [Fe/H] \rangle = -0.3$  (McWilliam & Rich 1994).

#### 4 DISCUSSION ON THE PROGENITOR MASSES OF PNE TOWARDS THE BULGE

The much smaller fraction of C-rich PNe in the bulge compared to the disk must reflect the change in the stellar populations between the two regions. The main factors that affect the production of C-rich PNe are the initial composition and the age of the stellar population; in old populations the stars sufficiently massive to produce C-rich PNe ( $\geq 1.5 M_\odot$ ) will have evolved beyond the PN stage. In this Section we examine the consequences of linking the progenitor population of PNe towards the bulge to the inner Galactic disk or to the bulge stellar population.

##### 4.1 Expected frequencies of C-rich PNe for various progenitor populations

It appears that the Galactic metallicity gradient is at the root of the trend for an increasing fraction of C-rich PNe beyond the solar circle (Casassus & Roche 2001, paper II), and it could be thought that a natural explanation for the rarity of C-rich bulge PNe may be an extrapolation of the Galactic disk trends to even more metal-rich environments. However, the distribution of oxygen abundances listed in Table 2 does not reach the required values. Also surprising is the fact that C-rich PNe, common in low metallicity environments, are found at rather high  $[O/H]$  in the bulge sample.

We now examine the consequences of assuming bulge PN progenitors have diffused off the inner galactic disk, but are otherwise similar to those of local PNe, and investigate the predictions of single star evolution using the synthetic AGB model proposed by Groenewegen & de Jong (1993), modified to include the results of Forestini & Charbonnel (1997, as described in paper II).

We considered three cases for the initial compositions of the progenitor population. The first two had initial metallicities normally distributed about  $Z = 0.02$  and  $Z = 0.03$ , with an arbitrary  $Z_{FWHM} = 0.005$ . The third had a distribution following the observed  $[O/H]$  distribution in the objects in our sample i.e. with  $\log(Z/0.02) \sim [O/H] = -0.3 \pm 0.4$  dex, and bounded by

$-1$  dex and  $+0.2$  dex. Initial compositions were approximated by a metallicity-scaled solar mix, except for O, for which we also considered  $^{16}O = ^{16}O_\odot (Z/0.02)^{1/7}$ , which is obtained by eliminating  $R$  from  $\log(Z/0.02) = -0.07(R - R_\odot)$  and  $\log(^{16}O/0.02) = -0.01(R - R_\odot)$  (the oxygen gradient inferred from B stars, as reported by Smartt et al. 2000).

A power law initial mass spectrum,  $p(M_i)dM_i \propto M_i^{-\kappa}dM_i$ , whose exponent  $\kappa$  was varied between 2 and 8, is taken to represent the progenitor population. The mass spectrum of PN progenitors is given by  $N(M) dM = \text{SFR}[t(M)] \text{IMF}(M) dM$  where  $t(M)$  is the time of birth for a progenitor of mass  $M$ . For a constant star formation rate (SFR), the Salpeter (1955) initial mass function (IMF) leads to  $\kappa = 2.35$ . For progenitors linked to the inner Galactic disk, in a conservative estimate the probability for a given star to diffuse off the plane would be proportional to the progenitor's lifetime, or about  $M^{-2}$ . Assuming randomly distributed star formation bursts behave on average as a constant SFR gives  $\kappa = 4.35$  for a Salpeter IMF. Actually, diffusion off the galactic disk is probably a cumulative process, and using the square of the lifetime may be more adequate, thereby giving  $\kappa = 6.35$ . Whether there were more/less bursts in the past than today<sup>†</sup> can be taken into account by increasing/decreasing  $\kappa$ . If the progenitors are coeval with globular clusters, then SFR is best approximated as a delta function at  $t = 0$ . We would have AGB stars at the  $0.8 M_\odot$  turnoff only (see below), and  $\kappa$  goes to infinity. However, this case is excluded by adopting a minimum initial mass of  $1.2 M_\odot$  for the progenitors of compact and IR-bright PNe, as in paper II, our purpose being to test whether the bulge and local PNe are similar stellar populations.

The resulting properties of the synthesised bulge PN population can be seen in Figure 3. The hypothesis that the bulge and local PNe are similar stellar populations predicts far too many C-rich objects in the bulge. Taking a  $Z$ -scaled solar mix (the thick lines) or  $C/O(Z)$  (the thin lines) does not significantly change the predictions. It would seem that even for the steepest  $\kappa$ , the bulge metallicities predict a majority of C-rich PNe. The only set of parameters which can account for the observed scarcity of C-rich objects within  $1-\sigma$  is  $Z = 0.03$ ,  $\kappa = 3.5 - 6$ , i.e. a super-metal-rich and fairly young population, derived from a constant SFR and having diffused off the inner disk.

It is also important to calculate the predicted frequency of C stars, which is observed to be very low in the Galactic bulge (see next Subsection). The predicted C/M star ratio on the thermally pulsing AGB, for  $\kappa = 2$ , may be considered an upper limit on the

<sup>†</sup> One underlying assumption is that the diffused population samples all masses, excluding the case of just one very recent burst (say in the inner 100 pc). The objects discussed here are distributed uniformly over the central  $10^\circ$ .



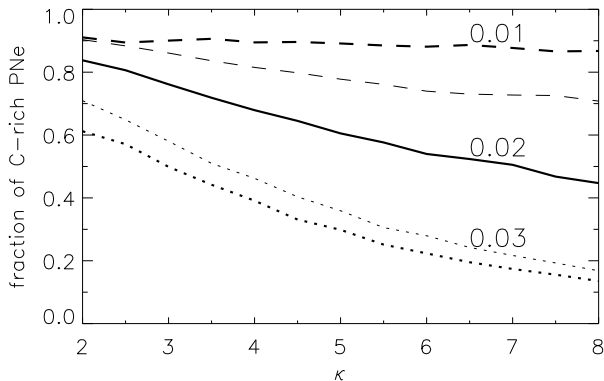


Figure 3: The predicted fraction of C-rich PNe as a function of  $\kappa$ , estimated by averaging the AGB mass loss composition over the last 2000 yr of evolution. The solid line corresponds to  $Z = 0.02$ , the dotted line to  $Z = 0.03$ , and the dashed line to the bulge metallicities (a broad distribution centred on  $Z = 0.01$ , see text). Thick and thin lines correspond respectively to initial compositions as in a  $Z$ -scaled solar mix, or taking into account  $C/O(Z)$ .

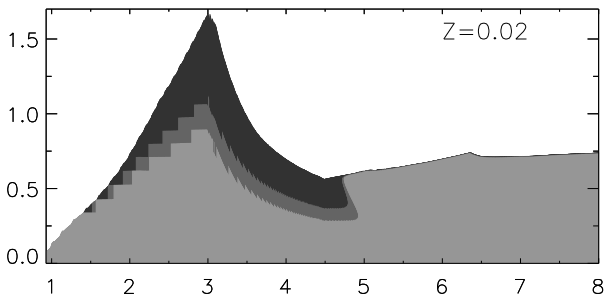


Figure 4: Time spent on the AGB ( $10^6$  years, in ordinates) as a function of initial mass (in  $M_{\odot}$ ), for the model presented in paper II (at solar metallicity). The grey scale grows darker from the M to S to C phases.

ratio that would be observed in the synthetic populations: M stars on the early AGB are bound to contaminate the star counts, and for a steeper  $\kappa$ , C stars are increasingly improbable. For  $Z = 0.03$ , the predicted ratio is  $C/M < 0.04$ , while for  $Z = 0.02$  we obtain  $C/M < 0.22$ , and  $C/M < 0.35$  for the bulge metallicities. Higher metallicities are associated with very low values of the  $C/M$  star ratio. The rarity of bulge C stars is naturally explained by their very short lifetimes, as illustrated in Figure 4. The very occurrence of this phase is sensitive to the progenitor’s mass, resulting from an interplay of mass loss in the stellar envelope and the thermal pulses (especially around  $\sim 2 M_{\odot}$ ).

N-enrichment is firmly established to be a function of progenitor mass, in the case of the Galactic disk population. Thus the statistics of N/O ratios suggests the bulge PNe are derived from a population similar in age to local PNe (if they have similar progeni-

tors). Although the highest N/O ratios, and hence the most massive progenitors, may be deficient in bulge PNe (Cuisinier et al. 2000), the upper end of the  $1\text{--}8M_{\odot}$  mass range is very infrequent, and derived differences with local PNe should be negligible (we avoid discussion of the predicted distribution of PN N/O ratios, as the frequency of N-enrichment in disk PNe is not understood, see Section 2.2 in paper II).

For single star evolution to account for the compositions of bulge PNe, a super-metal-rich and young progenitor population is required, i.e. an environment typical of the inner Galactic disk. But the oxygen abundances reported for bulge PNe, taken as one stellar population, are on average slightly subsolar, and similar to the disk objects. Thus, assuming the bulge and local PNe have similar progenitors (and assuming the reported  $[O/H]$  values are accurate), cannot reproduce the properties of the bulge sample when taken as one stellar population.

#### 4.2 Are the bulge PNe all type IV?

The overall picture gathered to date points at an old bulge, composed of stars no more massive than about  $0.8 M_{\odot}$  with significant scatter in metallicity about the solar value (Ortolani et al. 1995, Idiart et al. 1996, Bruzual et al. 1997, Barbuy, Bica & Ortolani 1998, Feltzing & Gilmore 2000). But this result is not unchallenged. Conclusions preferring a younger bulge have been reached (Holtzman et al. 1993, Kiraga, Paczynski & Stanek. 1997). In fact, although the results by Ortolani et al. (1995) have found strong support, they refer to the bulk of the bulge; some observations suggest the existence of an intermediate mass population<sup>‡</sup>. Frogel (1999) summarises his work on a bulge population less than  $\sim 1$  Gyr old: although there is no solid evidence for a young population in Baade’s window, a mix of young and old populations is found towards the inner bulge (fields less than  $1^{\circ}$  from the Galactic centre), as evidenced by an increase in luminous AGB stars.

A long standing problem related to the existence of an intermediate mass population in the bulge is the lack of C stars. Blanco, Blanco & McCarthy (1978) detected only one C star in 310 M stars. Azzopardi, Lequeux & Rebeiro (1991) reported a list of 33 C stars detected towards the bulge, but their properties are puzzling. Although the C stars share the same kinematics as bulge K and M giants, they are too faint to be on the AGB. The bulge C stars do not seem to be genuine AGB stars,

<sup>‡</sup> McWilliam and Rich (1994) estimate that the average mass of K giants in Baade’s window can be no less than  $1.1 M_{\odot}$ . The distribution of periods of LPV stars in the bulge has been interpreted as evidence for a population with ZAMS masses in excess of  $1.3 M_{\odot}$  (Harmon and Gilmore 1988), but this has recently been shown by Frogel & Whitelock (1998) to merely reflect a metallicity effect in an old population.

and could be dwarf C stars (dCs) along the line of sight to the bulge. dCs are observed to have low metallicities (Harris et al. 1998), and are most likely produced through binary evolution with  $Z < 0.5 Z_{\odot}$  (De Kool & Green 1995), making them members of the local population of spheroid dwarfs. Thus the lack of genuine AGB C stars is characteristic of the bulge.

The principal piece of information brought by the warm dust emission features of PNe in the direction of the bulge is that the proportion of C-rich nebulae is dramatically lower, only  $\sim 30\%$  against  $\sim 78\%$  in local PNe. In an extension of the method applied to disk PNe in papers I and II, we showed in section 4.1 that such a low fraction of C-rich nebulae and the nitrogen enrichment reported by Ratag et al. (1997) require a young and metal-rich population, with  $Z \sim 0.03$ . Yet on average the bulge and local PNe have similar metallicities, although the four C-rich object in the bulge sample are found at rather high  $[O/H]$ , and none is a definite bulge member.

Two alternatives should be considered:

(i) The bulge PNe with warm dust could be related to the type IV PNe in Peimbert's classification, i.e. halo PNe with peculiar abundances. The case of BB-1 (or PN G108.4-76.1), studied by Peña et al. (1993), merits attention as it is metal poor (O is underabundant relative to solar by one order of magnitude), has a velocity of  $\sim 200 \text{ km s}^{-1}$ , and is nonetheless enriched in carbon and nitrogen,  $\log(C/O) = +1$ ,  $\log(N/O) = +0.2$ .

(ii) The bulge PNe with warm dust are similar to the local population, but with higher metallicity and linked to the inner regions of the Galactic disk. A mechanism remains to be found by which such a population would diffuse off the Galactic plane.

Aspects of both alternatives seem applicable to the bulge PNe. The C-rich PNe are most likely metal-rich and foreground objects, and the lack of counterpart C stars is natural in metal-rich environments (the C phase would occur only at the very end of AGB evolution, and could possibly be linked with PN ejection).

Another piece of information is provided by the lack of metallicity dispersion in Baade's window M giants, about a mean slightly larger than the solar value (Frogel & Whitford 1987, Terndrup et al. 1991). The dispersion in metallicity for M giants is at most a factor of 2 in  $[Fe/H]$ , about  $\langle [Fe/H] \rangle = +0.3$ , in contrast with the large spread in metallicity of Baade's window K giants,  $\sim 1$  dex in  $[Fe/H]$  about  $\langle [Fe/H] \rangle = -0.3$ . Is the bulk of the M giants observed towards Baade's window from a young population, with uniformly high metallicity, linked to the inner Galactic disk?

Similar to the superposition of the populations traced by the K and M giants in Baade's window, there could be a superposition of two population in the bulge PNe, one linked to the inner disk and the other to the old bulge.

## 5 CONCLUSION

The C/O chemical balance for a sample of PNe towards the Galactic bulge has been established through the 8–13  $\mu\text{m}$  dust emission features. Out of 15 PNe with identified dust types, 4 PNe have C-based grains. The very low fraction of C-rich PNe is in contrast with the local PNe, and the bulge PNe probably form a different population. However, none of the C-rich PNe is an unquestionable bulge member. The fraction of C-rich nebulae among 'bona fide' bulge PNe could be much lower.

In the framework of single-star evolution, the properties of the bulge PN sample appear to be derived from a young and metal-rich population, linking the 'bulge' PNe to the inner Galactic disk. However, the distribution in metallicity of the bulge warm dust PNe follows that of Baade's window K giants, with a similar mean to solar neighbourhood PNe. It is difficult to reconcile the C/O balance inferred from the dust emission with a single bulge PN population. We are thus inclined to follow the suggestion by Peimbert (1992) that the bulge PNe are predominantly type IV, although contamination from Galactic disk objects is likely. In this context the C-rich PNe towards the bulge are linked to the inner Galactic disk, and the lack of counterpart C stars is a natural property of metal-rich environments.

We find that M 2-29, usually classified as a type IV PN with  $Z \sim 0.0008$ , shows silicate emission. It seems, however, that the ground-based  $[O/H]$  determinations could be in error (Torres-Peimbert et al. 1997). In the light of the significant uncertainties linked with the gas-phase abundances, discriminating between a bulge or a disk origin for 'bulge' PNe based on their  $[O/H]$  values may be premature. It would be interesting to obtain 8–13  $\mu\text{m}$  spectra of the 7 type IV PNe listed by Peimbert (1992) to investigate dust production at low metallicities.

## ACKNOWLEDGMENTS

We are grateful to the referee for an interesting report. S.C. acknowledges support from Fundación Andes and PPARC through a Gemini studentship.

## REFERENCES

- Acker A., Köppen J., Stenholm B., Raytchev B., 1991, AASS 89, 237
- Acker A., Ochsenbein F., Stenholm B., Tylenda R., Marcout J., Schohn C., 1992, 'The Strasbourg-ESO Catalogue of Galactic Planetary Nebulae', published by the European Southern Observatory
- Aitken D.K., Roche P.F., Spenser P.M., Jones B., 1979, ApJ, 233, 925
- Azzopardi M., Lequeux J., Rebeiro E., 1988, A&A, 202, L27
- Barbuy B., Bica E., Ortolani S., 1998, A&A, 333, 117
- Barlow M.J., 1983, IAU symp 103 "Planetary Nebulae" ed D.R. Flower p105

- Blanco B.M., Blanco V.M., McCarthy M.F., 1978, *nature* 271, 638
- Bruzual A.G., Barbuy B., Ortolani S., Bica E., Cuisinier F., Lejeune T., Schiavon R.P., 1997, *AJ*, 114, 1531
- Casassus S., Roche P.F., Aitken D.K., Smith C.H., 2001, *MNRAS*, 320, 424 (paper I)
- Casassus S., Roche P.F., 2001, *MNRAS*, 320, 435 (paper II)
- Ciardullo R., Jacoby G.H., Harris W.E., 1991, *ApJ*, 383, 487
- Cuisinier F., Maciel W.J., Köppen J., Acker A., Stenholm B., 2000, *A&A*, 353, 543
- De Kool M., Green P.J., 1995, *ApJ* 449, 236
- Durand S., Acker A., Zijlstra A., 1998, *A&AS*, 132, 13
- Faúndez-Abans M., Maciel W.J., 1987, *A&A*, 183, 324
- Feltzing S., Gilmore G., 2000, *A&A*, 355, 949
- Forestini M, Charbonnel C., 1997, *A&AS*, 123, 241
- Frogel J.A., 1999, in “Galaxy Evolution: Connecting the Distant Universe with the Local Fossil Record”, Invited Review, held September 1998, Observatoire de Paris-Meudon (astro-ph/9812034)
- Frogel J.A., Whitelock P.A., 1998, *AJ*, 116, 754
- Frogel J.A., Whitford A.E., 1987, *ApJ*, 320, 199
- Grevesse N., Anders E., 1989, ‘Cosmic Abundances of Matter’, AIP Conference Proceedings, 183, 1, Ed. C.J. Waddington, (New York: AIP)
- Groenewegen M.A.T, deJong T., 1993, *A&A*, 267, 410
- Harmon R., Gilmore G., 1988, 235, 1025
- Harris H.C., Dahn C.C., Walker R.L., Luginbuhl C.B., Monet A.K.B., Guetter H.H., Stone R.C., Vrba, F.J., Monet D.G., Pier J.R., 1998, *ApJ* 502, 437
- Holtzman J.A., Light R.M., Baum W.A., Worthey G., Faber S.M., Hunter D.A., O’Neil E.J.Jr., Kreidl T.J., Groth E.J., Westphal J.A., 1993, *AJ* 106, 1826
- Idiart T.P., de Freitas Pacheco J.A., Costa R.D.D., 1996, *AJ*, 111, 1169
- Kerr F.J., Lynden-Bell D., 1986, *MNRAS*, 221, 1023
- Kiraga M., Paczynski B., Stanek K.Z. 1997, *ApJ* 485, 611
- Kohoutek L., Pauls R., 1995, *A&AS*, 111, 493
- McWilliam A., Rich R.M., 1994, *ApJSS*, 1994, 91, 749
- Maciel W.J., 1984, *A&AS*, 55, 253
- Ortolani S., Renzini A., Gilmozzi R., Marconi G., Barbuy B., Bica E., Rich R.M., 1995, *nature*, 377, 701
- Peimbert M., 1978, in Terzian Y., ed., Proc. IAU Symp 76, ‘Planetary Nebulae’. Reidel, Dordrecht, p. 233
- Peimbert M., 1992, in ‘Observational Astrophysics’, Ed. R.E. White, IOP Publishing Ltd.
- Peña M., Stasińska G., Medina S., Ayala S., 1995, *RevMexAA*, 3, 233
- Ratag M.A., Pottash S.R., Dennefeld M, Menzies J., 1997, *A&ASS*, 126, 297
- Roche P.F., 1987, in ‘Planetary and Proto-Planetary Nebulae: From IRAS to ISO’, A. Preite Martinez (ed.), D. Reidel Publishing Company, p45
- Roche P.F., 1989, IAU symp 131 “Planetary Nebulae” ed S.Torres Peimbert, p117
- Salpeter E.E., 1955, *ApJ* 121, 161
- Schneider S. E., Terzian Y., Purgathofer A., Perinotto M., 1983, *ApJS*, 52, 399
- Terndrup D.M., Frogel J.A., Whitford A.E., 1991, *ApJ*, 378, 742
- Smartt S.J., Venn K.A., Dufton P.L., Lennon D.J., Rolleston W.R.J., Keenan F.P., 2000, *A&A*, *submitted* astro-ph/0009157
- Torres-Peimbert S., Dufour R. J., Peimbert M., Pena M., 1997, Proc IAU Symp. 180, ‘Planetary Nebulae’, p.281, eds H.J. Habing and H.J.G.L.M. Lamers
- Tylenda R., Stasińska G., Acker A., Stenholm B., 1991, *A&A*, 246, 221
- Van de Steene G.C., Zijlstra A.A., 1994, *A&AS*, 108, 485
- Webster B.L., 1988, *MNRAS*, 230, 377
- Wielen R., 1977, *A&A*, 60, 263
- Zijlstra A.A., Acker A., Walsh J.R., 1997, *A&AS*, 125, 289
- Zhang C.Y., 1995, *ApJSS*, 98, 659

This paper has been produced using the Royal Astronomical Society/Blackwell Science L<sup>A</sup>T<sub>E</sub>X style file.